

## Observation of the effects of phonon dispersion on the Fröhlich-interaction-induced second-order Raman scattering in $\text{Pb}_2\text{Sr}_2\text{PrCu}_3\text{O}_8$

M. Reedyk

*Max-Planck-Institut für Festkörperforschung, Heisenbergstrasse 1 70569 Stuttgart, Germany*

C. Thomsen

*Institut für Festkörperphysik, Technische Universität Berlin, Hardenbergstrasse 36, 10623 Berlin, Germany*

M. Cardona

*Max-Planck-Institut für Festkörperforschung, Heisenbergstrasse 1 70569 Stuttgart, Germany*

J.S. Xue\* and J.E. Greedan

*Department of Chemistry and Institute for Materials Research,  
McMaster University, Hamilton, Ontario, Canada L8S 4M1*

(Received 1 July 1994)

The one- and two-phonon Raman-scattering spectrum of single-crystal  $\text{Pb}_2\text{Sr}_2\text{PrCu}_3\text{O}_8$  is examined under resonance conditions. Strong features appear in the one-phonon spectrum at the positions of longitudinal optical (LO) infrared modes as the laser energy approaches that of the charge transfer gap. These Fröhlich-interaction-induced modes are accompanied by a second-order spectrum composed of overtones and combinations of the LO and ordinary Raman-allowed phonons. We examine the dependence on incident photon energy of both the line shape and center position of the highest frequency two-phonon feature, which can be unambiguously attributed to a pure overtone of an infrared LO vibration. Due to the two-phonon nature of the scattering process the crystal momentum  $\mathbf{q}$  is no longer restricted to small wave vectors and one can expect to observe effects of phonon dispersion. We find, indeed, changes in the line shape as the gap is approached, accompanied by a decrease in the center frequency to a value close to twice that of the  $\mathbf{q}\approx 0$  one-LO-phonon (1-LO) mode. A detailed comparison to the free electron theory for two-LO-phonon (2-LO) scattering by Zeyher [Phys. Rev. B **9**, 4439 (1974)] is carried out. Relationships between the effective lattice mass characterizing the dispersion of this LO branch and the electron and hole effective band masses are established, and an estimate of the effective electron and hole band masses is made based on the magnitude of the phonon dispersion in  $\text{YBa}_2\text{Cu}_3\text{O}_6$  as measured by neutron scattering experiments.

### I. INTRODUCTION

To date little attention has been focused on the second-order Raman-scattering spectrum of the cuprate superconductors. In contrast to the first-order spectrum where one is limited as a consequence of momentum conservation to phonons with  $\mathbf{q} \approx 0$ , the second-order spectrum allows participation of phonons from the entire Brillouin zone. In principle the corresponding spectra thus contain information concerning phonon dispersion. In practice the off-resonance second-order spectrum reflects the combined two-phonon density of states and it is difficult to extract information pertaining to a specific branch. Under resonance conditions, however, this generalization no longer strictly holds and it is sometimes possible to select scattering by specific modes. An example is the appearance, under resonance conditions, of longitudinal optical (LO) modes arising as a result of the  $\mathbf{q}$ -dependent Fröhlich interaction.<sup>1</sup>

Yoshida *et al.* have examined qualitatively the second-order Raman-scattering spectrum of various insulating

cuprates under resonance conditions and pointed out, by comparison with neutron-scattering dispersion curves, that several of the two-phonon features could be ascribed to scattering by large wave vector phonons.<sup>2</sup> There is, however, some disagreement on the nature of the strongly resonant second-order modes in  $\text{YBa}_2\text{Cu}_3\text{O}_6$ . First-order scattering by Fröhlich-interaction-induced LO phonons has previously been observed and identified in  $\text{YBa}_2\text{Cu}_3\text{O}_6$ .<sup>3</sup> Based on this finding, in a recent study Liu *et al.* attribute the strongly resonant two-phonon features to second-order scattering of Fröhlich-interaction-induced LO modes.<sup>4</sup> In contrast, Yoshida *et al.* argue that their results are inconsistent with an interpretation based on two-LO-phonon (2-LO) scattering, although the neutron-scattering branch to which they assign the modes to be second-order features of is labeled as being of a longitudinal nature.<sup>5</sup> Their claim is derived from the observations that the resonance behavior of lower-frequency second-order features is different from that of the highest-frequency mode and that the highest-frequency mode forms, near resonance, a shoulder. The

theory developed for 2-LO scattering by Zeyher,<sup>6</sup> and discussed in more detail below, is, however, not inconsistent with changes in the line shape of the second-order modes near resonance. Furthermore, the strength of the resonance at a given incident photon energy depends strongly on the LO phonon frequency—a lower-frequency mode being significantly farther away (detuned) from resonance at 2.71 eV than a higher-frequency mode when the gap is at 1.7 eV.

Herein we present a detailed study of the second-order Raman-scattering spectrum of  $\text{Pb}_2\text{Sr}_2\text{PrCu}_3\text{O}_8$  which is the insulating derivative of a high- $T_c$  superconductor with  $T_c \approx 70$  K obtained by partial substitution of the rare earth ion Pr by Ca.<sup>7</sup>  $\text{Pb}_2\text{Sr}_2\text{PrCu}_3\text{O}_8$  is structurally closely related to  $\text{YBa}_2\text{Cu}_3\text{O}_6$ , the difference being that in the former compound the oxygen-free Cu(1) layer is sandwiched between two additional PbO layers. We find upon tuning the incident photon energy to values approaching the charge-transfer (CT) gap of  $\text{Pb}_2\text{Sr}_2\text{PrCu}_3\text{O}_8$  that new modes corresponding to the LO frequencies of infrared-active modes appear in the Raman spectrum. We focus our attention, rather, on the second-order spectrum, where pronounced changes occur in the intensity, "center" position and line shape of the observed modes. We find that in this case as well, the results can be interpreted in terms of scattering by 2-LO phonons. We attempt a detailed comparison to the theory of Ref. 6 which shows that the shift of the center position, and the accompanying changes in line shape arise from dispersion in the LO phonon branch.

## II. EXPERIMENTAL DETAILS

The single-crystal sample used in our investigation was synthesized via a PbO/NaCl flux technique described previously.<sup>8</sup> The Raman spectra, collected using a Dilor triple spectrometer with a charge coupled device (CCD) multichannel detector, were measured in a nearly backscattering configuration with  $\mathbf{k}_i \parallel \mathbf{k}_s \parallel c$  axis and  $\mathbf{E}_i \parallel \mathbf{E}_s \parallel x'$  (or  $y'$ ). Here  $x'$  is a direction  $45^\circ$  between that of the  $a$  and  $b$  axes so that phonons of both  $A_{1g}$  and  $B_{1g}$  symmetry could be observed<sup>9</sup> and  $z$  is along the  $c$  axis of the crystal.  $\mathbf{k}$  and  $\mathbf{E}$  represent the pseudomomentum and electric field vector, respectively, of the incident ( $i$ ) and scattered ( $s$ ) light. The resonance behavior was investigated at room temperature by measuring with discrete lines of Ar and Kr ion lasers lying between 457.9 and 752.5 nm. The measured spectra were carefully corrected for detector and spectrometer response, transmission at the sample-vacuum interface, effective scattering volume, and the effective solid angle of collection.

## III. RESULTS

In Fig. 1(a) we show the high-frequency imaginary dielectric function of  $\text{Pb}_2\text{Sr}_2\text{PrCu}_3\text{O}_8$  for  $\mathbf{E} \parallel a, b$  obtained by Kramers-Kronig (KK) analysis of reflectance data.<sup>10</sup> The CT excitation, common to all insulating derivatives

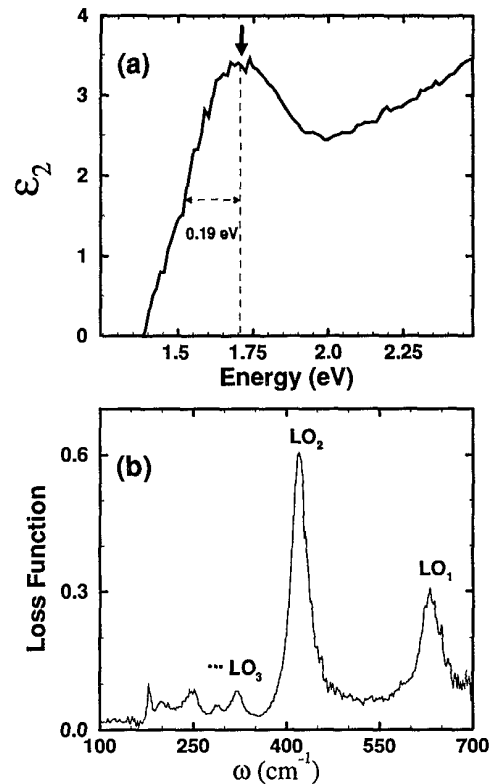


FIG. 1. Kramers-Kronig-derived optical properties of  $\text{Pb}_2\text{Sr}_2\text{PrCu}_3\text{O}_8$  for  $\mathbf{E} \parallel a, b$ . (a) High-frequency imaginary dielectric function (solid curve) showing the charge-transfer excitation centered at 1.71 eV (arrow). The dashed lines show how the lifetime broadening is estimated. (b) Low-frequency dielectric loss function. Peaks give the position of LO modes. Adapted from Ref. 10.

of the cuprate superconductors,<sup>11,12</sup> is clearly observed. Note that its center position (1.71 eV, marked by an arrow) is almost identical to that in  $\text{YBa}_2\text{Cu}_3\text{O}_6$ .<sup>12</sup> As illustrated in the figure its lifetime broadening (half width, half maximum) is estimated to be 0.19 eV.

Figure 2 shows a set of three Raman spectra at different incident laser energies. In contrast to the Raman-allowed  $B_{1g}$  mode at 278  $\text{cm}^{-1}$ , the modes at 435 and 644  $\text{cm}^{-1}$  show strongly resonant behavior as the incident laser energy approaches that of the CT excitation. We attribute their presence to the intraband Fröhlich interaction which results in the appearance, under resonance conditions, of Raman dipole-forbidden infrared LO modes. Figure 1(b) shows the dielectric loss function of  $\text{Pb}_2\text{Sr}_2\text{PrCu}_3\text{O}_8$  in the 100–700  $\text{cm}^{-1}$  phonon energy region for  $\mathbf{E} \parallel a, b$ ; also obtained by KK analysis of reflectance data.<sup>10</sup> The peaks approximate the positions of infrared LO modes; the two most prominent ones at 421 and 631  $\text{cm}^{-1}$  correspond closely to the strongly resonant modes observed in the Raman spectra.

In Fig. 2 several broader two-phonon features are also observed. Labeling the one-phonon modes at 644 and 435  $\text{cm}^{-1}$  as  $\text{LO}_1$  and  $\text{LO}_2$ , respectively, one finds that the second-order features near 840, 1050, and 1300  $\text{cm}^{-1}$  can be assigned to  $2\text{-LO}_2$ ,  $\text{LO}_1 + \text{LO}_2$ , and  $2\text{-LO}_1$ , re-

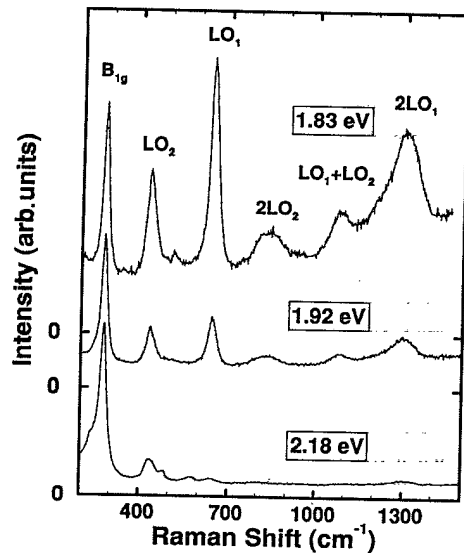


FIG. 2. One- and two-phonon Raman scattering spectra of  $\text{Pb}_2\text{Sr}_2\text{PrCu}_3\text{O}_8$  at different incident laser energies. Note that the  $B_{1g}$  mode maintains approximately the same intensity in all three spectra while the one-phonon modes at  $435$  and  $644$   $\text{cm}^{-1}$  ( $\text{LO}_2$ ,  $\text{LO}_1$ ), as well as all of the two-phonon features, show strongly resonant behavior.

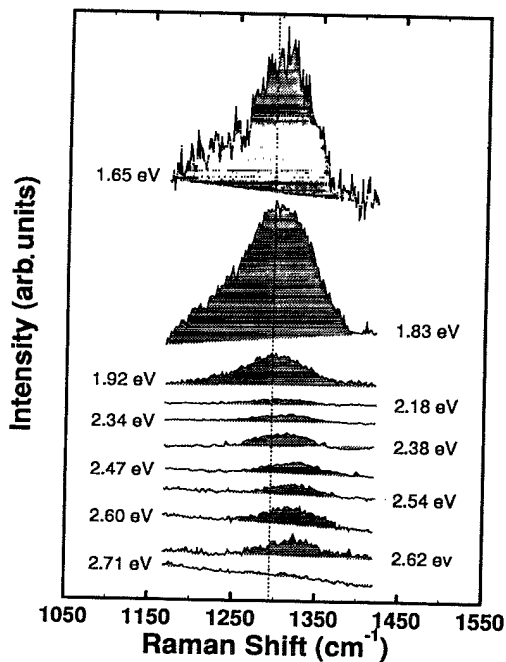


FIG. 3. Resonance behavior of the highest-frequency two-phonon feature of  $\text{Pb}_2\text{Sr}_2\text{PrCu}_3\text{O}_8$ . Note in addition to the changes in intensity that the "center" position shifts down by approximately  $30$   $\text{cm}^{-1}$  as the incident laser energy is varied from  $2.71$  to  $1.83$  eV. Note as well the pronounced asymmetry of the mode near resonance.

spectively. A more detailed analysis indicates that the Raman-allowed  $A_{1g}$  and  $B_{1g}$  modes at  $150$  and  $278$   $\text{cm}^{-1}$  also contribute to the two-phonon spectrum in combination with the LO modes so that only the highest-frequency feature near  $1300$   $\text{cm}^{-1}$  can be unambiguously assigned to a purely 2-LO overtone process. We thus further focus our attention on this mode.

In Fig. 3 we show this mode for a series of different incident laser energies. Of interest is not only the strongly resonant behavior of the intensity as the CT gap is approached, but also the downward shift in the frequency of the maximum and the accompanying changes in line shape. The experimental curves were fitted with one or more Lorentzians, as deemed necessary to account for asymmetry, and the fitted curve was used to determine the frequency at which the maximum occurs, and the magnitude of the full width at half maximum. In Fig. 4 we plot (open circles) the dependence of these quantities on incident energy. As we show next, the trends

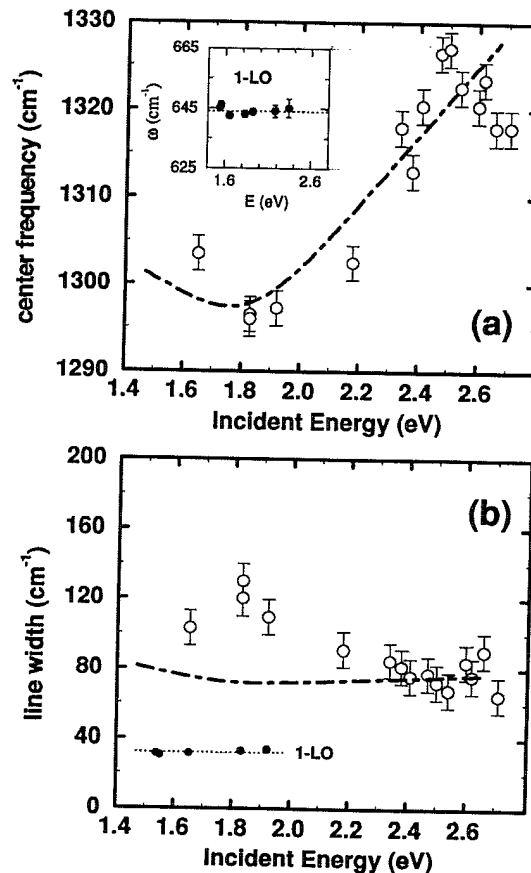


FIG. 4. Variation in the position of the maximum (a) and in the full width at half maximum (b) with incident laser energy (open symbols). Also shown (solid symbols) are the linewidth and the center frequency [inset to (a)] of the corresponding 1-LO mode. The 1-LO data do not extend over the entire energy range because the one-phonon feature becomes too weak to detect off resonance. The dashed curves show a comparison to the theory of Zeyher (revised to allow for lifetime broadening as discussed in the text) for the set of parameters given in Table I.

observed in Fig. 4 can be understood as arising from the dispersion in the LO phonon branch.

#### IV. DISCUSSION

The forbidden first-order intraband Fröhlich interaction results from an expansion in the components of  $\mathbf{q}$  of the matrix element describing the long-range contribution to the electron-phonon Hamiltonian. [The short-range interaction gives rise to the deformation potential associated with transverse optical (TO) modes.] The Fröhlich Hamiltonian  $H_F$  is given by

$$H_F = \frac{C_F}{|\mathbf{q}|} (e^{i\frac{\mu}{m_e}\mathbf{q}\cdot\mathbf{r}} - e^{i\frac{\mu}{m_h}\mathbf{q}\cdot\mathbf{r}}), \quad (1)$$

where  $C_F$  is the Fröhlich coupling constant.<sup>1</sup> Here  $m_e$  and  $m_h$  are the effective band masses of the electron and hole, respectively,  $\mu$  is the reduced mass, and  $\mathbf{r}$  is the coordinate for the relative motion of the electron and hole.

Upon expansion in  $\mathbf{q}$  of the exponentials in Eq. (1) the first term (proportional to  $1/|\mathbf{q}|$  due to the prefactor) cancels as a result of equal and opposite contributions from the electron and hole. The second term ( $|\mathbf{q}|$  independent), also called the *interband* Fröhlich interaction because it is nonzero only for transitions between different bands, contributes to first-order LO scattering in noncentrosymmetric crystals. The third term, proportional to  $|\mathbf{q}|$ , is the nonvanishing form of lowest order when there is a center of inversion as is the case in the cuprates, and describes first-order *intraband* scattering of LO phonons. Because it is zero for  $\mathbf{q} = 0$  this term is often referred to as dipole "forbidden." Under resonance conditions, however, this term can become considerable even for the small  $\mathbf{q}$  imparted to the phonon by the incident photon in a first-order process.

Because in a second-order process the two phonons can conserve crystal momentum by carrying, in the limit of zero wave vector for the photon, equal and opposite  $\mathbf{q}$ 's of any magnitude, the Fröhlich-interaction-induced second-order scattering, which is also expected to show a strong resonant enhancement near the gap, is however not dipole "forbidden" off resonance. Furthermore, a clear separation into inter- and intraband terms is no longer possible. Zeyher has calculated the second-order Raman efficiency for  $\mathbf{q}$ -dependent Fröhlich coupling in a two-band model with parabolic bands and free electron-hole pairs as the excited states.<sup>6</sup> His calculation takes the full  $\mathbf{q}$  dependence [Eq. (1)] of the Fröhlich interaction into account. In addition to calculating the resonance behavior of the total cross section  $d\sigma/d\Omega$ , which gives the absolute scattering intensity as a function of incident excitation energy, he provides, assuming parabolic dispersion for the phonon branch, an expression for the differential scattering cross section,  $d^2\sigma/d\Omega d\omega'$ , which gives for a specified incident excitation energy  $\hbar\omega_L$  the distribution of the Raman-shifted photon frequencies  $\omega'$ . The position of the maximum of this function is thus defined to be the "center" position of the 2-LO-phonon mode and the full width at half maximum, the linewidth. In his calcu-

lation Zeyher considers only broadening due to phonon dispersion. We added to that a Lorentzian broadening to account for the natural lifetime of the mode; that is, we use for the momentum dependence of the optical phonons

$$\hbar\Omega_{LO}(q) = \hbar\Omega_{LO}(0) - i\frac{\Gamma_{LO}}{2} + \frac{\hbar^2 q^2}{2M_{LO}}, \quad (2)$$

different from the form used by Zeyher<sup>6</sup> only in the addition of the term  $-i\Gamma_{LO}/2$ . In Eq. (2),  $q$  is the magnitude of  $\mathbf{q}$ ,  $\hbar\Omega_{LO}(0)$  and  $\Gamma_{LO}$  are the ( $q=0$ ) 1-LO-phonon energy and full width at half maximum, respectively, which can be determined experimentally from the first-order Raman scattering spectrum,  $\hbar\Omega_{LO}(q)$  is the  $q$ -dependent phonon energy, and  $M_{LO}$  is a vibrational "effective mass" determining the magnitude of the dispersion. The sign of the term quadratic in  $q$  is chosen to agree with the sign of the experimentally observed shifts in the center frequency of the 2-LO<sub>1</sub> mode. The differential scattering cross section for intraband 2-LO Fröhlich scattering is then given for a Stokes process by

$$\frac{d^2\sigma}{d\Omega d\omega'} \propto \int_0^\infty dy \frac{I\left(\sqrt{\frac{M_{LO}}{2\mu\hbar\Omega_{LO}(0)}}y}\right)}{\sqrt{y}} \times \left[ \frac{\Gamma_{LO}}{[y - \hbar\omega_L + \hbar\omega' + 2\hbar\Omega_{LO}(0)]^2 + \Gamma_{LO}^2} \right], \quad (3)$$

where  $I(y)$  is given by Eq. (27) of Ref. 6. Because we are interested only in the position of the maximum and the width at half maximum, we omit in Eq. (3), and our subsequent numerical evaluation thereof, all constant multiplicative prefactors.

Equation (3) thus represents a calculation of the Raman scattering *spectrum* of the 2-LO mode including lifetime broadening. We thus evaluated Eq. (3) for various incident laser energies, and selected from the results the frequency at which the maximum occurs, and the corresponding full width at half maximum. The dashed lines in Fig. 4 show the values obtained for these quantities as a function of incident energy for the set of parameters given in Table I. There is quite good agreement between theory and experiment for the position of the maximum, as well as for the magnitude of the linewidth of the two-phonon feature well above resonance. We point out that the 1-LO-phonon frequency, and linewidth, and the energy and lifetime broadening of the exciton are fixed from experiment. This leaves only the three effective masses as "free" parameters.

TABLE I. Parameters used for the fit shown in Fig. 4. Here  $m_e$  and  $m_h$  are the electron and hole effective band masses, respectively,  $m$  is the free electron rest mass,  $\Omega_{LO}(0)$  and  $\Gamma_{LO}$  are the center frequency and full width at half maximum of the 1-LO phonon Raman-line,  $M_{LO}$  is an effective mass describing the magnitude of the 1-LO-phonon dispersion, and  $E_g$  and  $\eta$  correspond to the characteristic energy and lifetime broadening of the exciton (CT excitation).

$m_e$	$m_h$	$\Omega_{LO}(0)$	$\Gamma_{LO}$	$M_{LO}$	$E_g$	$\eta$
$0.085m$	$0.218m$	$644 \text{ cm}^{-1}$	$32 \text{ cm}^{-1}$	$100m$	$1.71 \text{ eV}$	$0.19 \text{ eV}$

The above set of effective mass parameters is nevertheless not unique. In order to explore the relationship between the three effective masses we chose various values of  $M_{LO}$  and attempted to reproduce, as closely as possible, the fit shown in Fig. 4. The experimentally determinable parameters [ $\Omega_{LO}(0)$ ,  $\Gamma_{LO}$ ,  $E_g$ , and  $\eta$ ] retained for this procedure their values listed in Table I. We found for a given value of  $M_{LO}$  that  $m_e$  and  $m_h$  are determined uniquely in order to reproduce the magnitude and slope of the incident energy dependence of the center position, as well as the overall magnitude of the off-resonance 2-LO linewidth which is larger than twice that of the 1-LO mode. (We comment below on our inability to fit the 2-LO linewidth near resonance.) In Fig. 5 we show the results of this numerical investigation. Note that logarithmic scales are used in order to display the results over a wide range of values of  $M_{LO}$ . From the main figure we conclude for  $M_{LO} > 100m$  that  $m_e$  depends linearly on  $M_{LO}$ . Some deviation from linearity is observed for values of  $M_{LO}$  less than  $100m$ . The intercept of the linear region is zero within uncertainty. From the figure inset we see that for  $M_{LO} > 100m$  the ratio  $m_e/m_h$  is essentially constant with a value  $\approx 0.39$ . Below  $M_{LO} \approx 100m$  the ratio of  $m_e$  to  $m_h$  increases rapidly and asymptotically towards a value of 1.

Thus a unique set of parameters can be defined if the effective lattice-mass characterizing the phonon dispersion is known. It has been established in the literature that 2-LO scattering in correlated systems is limited to  $q$ 's such that  $2\pi/q$  is larger than the Bohr ra-

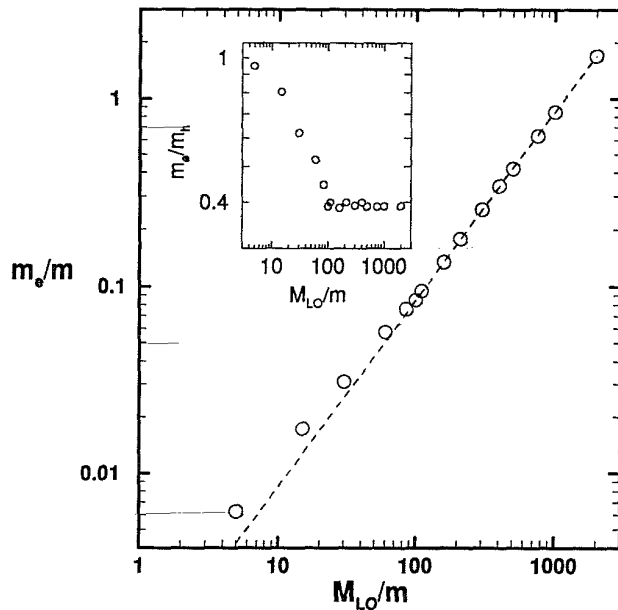


FIG. 5. Relationships between the effective lattice mass characterizing the dispersion of the LO band ( $M_{LO}$ ) and the electron ( $m_e$ ) and hole ( $m_h$ ) effective band masses determined numerically for parameters corresponding to  $Pb_2Sr_2PrCu_3O_8$  as discussed in the text. Note for  $M_{LO} > 100m$  that  $m_e$  varies linearly with  $M_{LO}$  (slope  $\approx 8.5 \times 10^{-4}$ , intercept  $\approx 0$ ) and that  $m_e/m_h$  takes on a constant value of  $\approx 0.39$ .

dius of the exciton.<sup>13</sup> This implies that one is usually probing only dispersion near the zone center and justifies a parabolic approximation such as Eq. (2). Although we have not considered excitonic effects, we assume that this observation holds here also. The phonon dispersion of the highest-frequency LO mode in  $YBa_2Cu_3O_6$  which is assigned, as is the mode we are investigating in  $Pb_2Sr_2PrCu_3O_8$ , to an in-plane bond-stretching vibration of Cu and O has been measured along the [100] and [110] directions using neutron-scattering.<sup>5</sup> For the [100] direction, a parabolic fit to the data near the zone center yields an effective vibrational mass between  $45m$  and  $60m$  (depending on the range of the Brillouin zone used in the fit) while for the [110] direction a value between  $30m$  and  $35m$  is estimated. In both cases the range of  $q$  used covers shifts of the magnitude and sign observed in our measurements. For values of  $M_{LO}$  between  $30m$  and  $60m$ , corresponding to those relevant for  $YBa_2Cu_3O_6$ , we find that  $m_e$  takes on values between  $0.03m$  and  $0.06m$ , respectively, while  $m_h$  varies between  $0.05m$  and  $0.11m$ , respectively. If the phonon dispersion for  $Pb_2Sr_2PrCu_3O_8$  is smaller than that of  $YBa_2Cu_3O_6$ , the effective band masses will increase in accordance with the results of Fig. 5. For comparison we mention that for a typical bulk semiconductor the dispersion near the  $\gamma$  point is very small, and hence the effective vibrational mass is quite large; for example, in GaP,  $M_{LO} = 720m$ .<sup>6</sup> The corresponding shifts in the center frequency and changes in the linewidth due to dispersion in GaP are in this case calculated, using parameters relevant for GaP and a detuning from the gap similar to that used in our study of  $Pb_2Sr_2PrCu_3O_8$ , to be of the order  $1 \text{ cm}^{-1}$  and hence almost indistinguishable within experimental uncertainty (a combination of resolution and the relative accuracy with which zero shift can be determined).<sup>14</sup> For this reason, no attempt to compare experimental shifts and linewidth changes to the theory of Zeyher has to our knowledge been made before now, although shifts of the order  $1.5 \text{ cm}^{-1}$  were observed in GaAs and attributed to phonon dispersion,<sup>15</sup> and pronounced changes in the line shape of 2-LO modes near resonance were noted in various semiconductors.<sup>16</sup>

We note from Fig. 4 that for incident energies near and below the gap the agreement between theory and experiment, especially for the case of the linewidth, is poor. This is likely caused by the neglect of correlation effects. Correlation contributes a significant enhancement to the scattering cross section. That is, compared to the uncorrelated particle-hole pair which is free to scatter in any direction before recombining, the correlated pair is "bound" together with a characteristic distance of the Bohr radius of the exciton. The probability for recombination in the coherent Raman-scattering process is thus much higher in the second case, resulting in an enhanced scattering cross section. Far from resonance, above the gap, one is dealing mainly with states of the electronic continuum. Near the gap, however, the discrete states of the correlated system play a dominant role and should be taken into account.

Unlike semiconductors where the effective band masses are known quite accurately from experiment (e.g., cy-

clotron resonance) in the cuprates they have thus far remained largely undetermined. In semiconductor systems incorporation of electron-hole correlation into the theory for 2-LO scattering has proven to be very successful in modeling the shape of the observed *integrated intensity* profile (i.e.,  $d\sigma/d\Omega$  as a function of  $\hbar\omega_L$ ) using only parameters known from experiment,<sup>17</sup> although some discrepancies in absolute value were still found. Accurate determination of the absolute intensity (usually involving comparison to a known standard such as BaF<sub>2</sub>) is, however, significantly more difficult than determining as a function of incident photon energy ( $\hbar\omega_L$ ) shifts in the frequency of the maximum of the phonon profile (i.e.,  $d^2\sigma/d\Omega d\omega'$  as a function of  $\omega'$ ). Thus, with more exact information for the effective vibrational mass from neutron-scattering studies, and a theory incorporating electron-hole correlation, this technique of following changes in the position of the center frequency and linewidth of the 2-LO-phonon Raman line, an option unavailable to studies involving semiconductor systems due to the flatness of their phonon dispersion, may serve for the cuprates and other materials with sizable LO phonon dispersion as a valuable means of obtaining information concerning effective band masses.

## V. CONCLUSION

We have shown that a downward shift of the center frequency of the highest-frequency 2-LO-phonon Raman

line of Pb<sub>2</sub>Sr<sub>2</sub>PrCu<sub>3</sub>O<sub>8</sub> to a value close to twice that of the  $q \approx 0$  1-LO mode as the CT gap is approached, as well as the magnitude of the off-resonance linewidth which is greater than twice that of the 1-LO mode, can be attributed to dispersion in the LO phonon branch. Because the size of the dispersion is noticeably larger than in typical bulk semiconductors such as GaP, where its effect on the linewidth and center frequency is within experimental uncertainty almost negligible, it is proposed that with some refinement in the theoretical approach this could become a useful means of obtaining information concerning the electronic structure (e.g., effective band masses) of the insulating cuprates. However, since our fitting procedure has been optimized for the off-resonance behavior, where the continuum states dominate and the free electron theory is most valid, we suggest that the present results represent a reasonable estimate.

## ACKNOWLEDGMENTS

Helpful discussions with A. Cantarero, E.J. Nicol, C. Trallero-Giner, and R. Zeyher, as well as technical assistance from H. Hirt, M. Siemers, and P. Wurster are gratefully acknowledged. One of the authors (M.R.) would like to thank the Max-Planck-Gesellschaft and the Natural Sciences and Engineering Research Council (NSERC) of Canada for financial support. This work has been supported in part by Human Capital and Mobility Grant No. ERBSC1\*CT910751 of the European Union.

\* Present address: Argonne National Laboratory, 9700 Cass Ave., Argonne, IL 60439.

<sup>1</sup> M. Cardona, in *Topics in Applied Physics (Light Scattering in Solids II)*, edited by M. Cardona and G. Güntherodt (Springer-Verlag, Berlin, 1982), Vol. 50, pp. 128-135.

<sup>2</sup> M. Yoshida, S. Tajima, N. Koshizuka, S. Tanaka, S. Uchida, and T. Itoh, *Phys. Rev. B* **46**, 6505 (1992).

<sup>3</sup> E.T. Heyen, J. Kircher, and M. Cardona, *Phys. Rev. B* **45**, 3037 (1992).

<sup>4</sup> Ran Liu, S.L. Cooper, M.V. Klein, W.C. Lee, S-W. Cheong, and D.M. Ginsberg (unpublished).

<sup>5</sup> L. Pintschovius, N. Pyka, W. Reichardt, A.Yu. Rumiantssev, N.L. Mitrofanov, A.S. Ivanov, G. Collin, and P. Bourges, *Physica C* **185-189**, 156 (1991).

<sup>6</sup> R. Zeyher, *Phys. Rev. B* **9**, 4439 (1974).

<sup>7</sup> L.F. Schneemeyer, R.J. Cava, A.C.W.P. James, P. Marsh, T. Siegrist, J.V. Waszczak, J.J. Krajewski, W.P. Peck, Jr., R.L. Opila, S.H. Glarum, J.H. Marshall, R. Hull, and J.M. Bonar, *Chem. Mater.* **1**, 548 (1989).

<sup>8</sup> J.S. Xue, M. Reedyk, J.E. Greedan, and T. Timusk, *J. Solid State Chem.* **102**, 492 (1993).

<sup>9</sup> Ran Liu, M. Cardona, B. Gegenheimer, E.T. Heyen, and C. Thomsen, *Phys. Rev. B* **40**, 2654 (1989).

<sup>10</sup> M. Reedyk, Ph.D. thesis, McMaster University, 1992.

<sup>11</sup> T. Arima, K. Kikuchi, M. Kasuya, S. Koshihara, Y.

Tokura, T. Ido, and S. Uchida, *Phys. Rev. B* **44**, 917 (1991).

<sup>12</sup> S.L. Cooper, G.A. Thomas, A.J. Millis, P.E. Sulewski, J. Orenstein, D.H. Rapkine, S-W. Cheong, and P.L. Trevor, *Phys. Rev. B* **42**, 10795 (1990).

<sup>13</sup> J.F. Scott, R.C.C. Leite, and T.C. Damen, *Phys. Rev.* **188**, 1285 (1969).

<sup>14</sup> Note that in Ref. 6 there are errors in the numerical evaluation of the scattering cross sections depicted in the figures. Our work is in agreement with the results of Ref. 17 for the free electron theory (FET). In particular we point out that in Figs. 5 and 6 of Ref. 6 the frequency scale for the shift and width is approximately a factor of 6 too large. The smaller values we find in attempting to reproduce these figures are in agreement with experiment on typical semiconductor systems (see, e.g., Ref. 15).

<sup>15</sup> D. Olego and M. Cardona, *Solid State Commun.* **39**, 1071 (1981).

<sup>16</sup> T.C. Damen, R.C.C. Leite, and J. Shah, in *Proceedings of the Tenth International Conference on the Physics of Semiconductors*, edited by S.P. Keller, J.C. Hensel, and F. Stern (United States Atomic Energy Commission, Washington, D.C., 1970), p. 735.

<sup>17</sup> A. García-Cristóbal, A. Cantarero, C. Trallero-Giner, and M. Cardona, *Phys. Rev. B* **49**, 13430 (1994).